Destabilization of DJ-1 by Familial Substitution and Oxidative Modifications: Implications for Parkinson's Disease†

John D. Hulleman,‡ Hamid Mirzaei,§,▽,# Emmanuel Guigard,||,# Kellie L. Taylor,‡,# Soumya S. Ray,⊥ Cyril M. Kay,|| Fred E. Regnier,§ and Jean-Christophe Rochet*,‡

Department of Medicinal Chemistry and Molecular Pharmacology, Purdue University, West Lafayette, Indiana 47907, Department of Chemistry, Purdue University, West Lafayette, Indiana 47907, Department of Biochemistry, University of Alberta, Edmonton, Alberta, Canada T6G 2H7, and Harvard Center for Neurodegeneration and Repair and Department of Neurology, Harvard Medical School, Boston, Massachusetts 02115

Received January 29, 2007; Revised Manuscript Received March 16, 2007

ABSTRACT: Parkinson's disease (PD) is a neurodegenerative disorder characterized by oxidative stress and protein aggregation. Both toxic phenomena are mitigated by DJ-1, a homodimeric protein with proposed antioxidant and chaperone activities. The neuroprotective function of DJ-1 is modulated by oxidation of cysteine 106, a residue that may act as an oxidative stress sensor. Loss-of-function mutations in the DJ-1 gene have been linked to early onset PD, and age-dependent over-oxidation of DJ-1 is thought to contribute to sporadic PD. The familial mutant L166P fails to dimerize and is rapidly degraded, suggesting that protein destabilization accounts for the dysfunction of this mutant. In this study, we investigated how the structure and stability of DJ-1 are impacted by two other pathogenic substitutions (M26I and E64D) and by over-oxidation with H_2O_2. Whereas the recombinant wild-type protein and E64D both adopted a stable dimeric structure, M26I showed an increased propensity to aggregate and decreased secondary structure. Similar to M26I, over-oxidized wild-type DJ-1 exhibited reduced secondary structure, and this property correlated with destabilization of the dimer. The engineered mutant C106A had a greater thermodynamic stability and was more resistant to oxidation-induced destabilization than the wild-type protein. These results suggest that (i) the M26I substitution and over-oxidation destabilize dimeric DJ-1, and (ii) the oxidation of cysteine 106 contributes to DJ-1 destabilization. Our findings provide a structural basis for DJ-1 dysfunction in familial and sporadic PD, and they suggest that dimer stabilization is a reasonable therapeutic strategy to treat both forms of this disorder.

Parkinson's disease (PD[1]) is a neurodegenerative disorder caused by the selective loss of dopaminergic neurons from the s*ubstantia nigra* (*1*). A pathological hallmark of surviving dopaminergic neurons is the presence of Lewy bodies, dense cytosolic inclusions that contain a variety of aggregated proteins and are enriched with fibrillar α-synuclein (*2*). Mitochondria from PD patients exhibit a decrease in the activity of complex I in the electron transport chain (*3*). This decrease in complex I activity causes a buildup of reactive oxygen species (ROS) in affected neurons, ultimately triggering damage to DNA, lipids, and proteins (*3*−*5*). Dopaminergic neurons are thought to be selectively vulnerable to oxidative stress because they have high basal levels of ROS from the metabolism and auto-oxidation of dopamine (*3*).

A number of patients with early onset PD have homozygous, autosomal recessive mutations in the gene encoding DJ-1. These mutations include a six-exon deletion (*6*) and missense mutations encoding the DJ-1 variants M26I (*7*), E64D (*8*), and L166P (*6*). Evidence from cell-culture studies suggests that DJ-1 protects neurons via an antioxidant function (*9*, *10*). DJ-1 knockout mice show nigrostriatal dopaminergic deficits (*11*−*13*) and are hypersensitive to the toxic effects of MPTP (*13*). Studies involving DJ-1 loss-of-

† This work was supported by grants from the Purdue Research Foundation (J-CR), American Parkinson Disease Association (J-CR), National Parkinson Foundation (J-CR, FER), American Foundation for Pharmaceutical Education (JDH), Protein Engineering Network of Centres of Excellence (CMK), and Alberta Cancer Board (CMK). The research described herein was conducted in a facility constructed with support from Research Facilities Improvement Program Grants Number C06-14499 and C06-15480 from the National Center for Research Resources of the National Institutes of Health (Department of MCMP, Purdue University).

* To whom correspondence should be addressed. Tel: (765) 494-1413. Fax: (765) 494-1414. E-mail: rochet@pharmacy.purdue.edu.

‡ Department of Medicinal Chemistry and Molecular Pharmacology, Purdue University.

§ Department of Chemistry, Purdue University.

|| University of Alberta.

⊥ Harvard Medical School.

# These authors contributed equally to this work.

▽ Present address: Institute for Systems Biology, Seattle, WA 98103.

[1] Abbreviations: BCA, bicinchoninic acid; DMF, *N*,*N*-dimethylformamide; DSS, disuccinimidyl suberate; DTT, dithiothreitol; far-UV CD, far-ultraviolet circular dichroism; HEPES, 4-(2-hydroxyethyl)piperazine-1-ethanesulfonic acid; IEF, isoelectric focusing; IPTG, isopropyl-*β*-D-thiogalactopyranoside; KP_i, potassium phosphate; LB, Luria−Bertani broth; LC-MS/MS, liquid chromatography-tandem mass spectrometry; 2ME, 2-mercaptoethanol; MWCO, molecular weight cut off; PBS, phosphate buffered saline; PCR, polymerase chain reaction; PMSF, phenylmethylsulfonyl fluoride; ROS, reactive oxygen species; SDS−PAGE, sodium dodecyl sulfate−polyacrylamide gel electrophoresis; SEC, size-exclusion chromatography; Tris, Tris(hydroxymethyl)aminomethane.

10.1021/bi7001778 CCC: $37.00
Published on Web 04/24/2007

function flies also show an increase in dopaminergic cell death upon challenge by oxidative insults (*14*−*16*). DJ-1 converts to more acidic isoforms in mammalian cells treated with pro-oxidants (*17*−*19*) and in the brains of rats exposed to the complex I inhibitor rotenone (*20*). The conversion of DJ-1 to acidic isoforms results at least in part from the oxidation of cysteine to cysteine sulfinic acid at position 106 (*18*, *19*). The antioxidant function of DJ-1 may depend on the association of the protein with mitochondria (*18*, *21*, *22*), and evidence from one group suggests that the oxidation of cysteine 106 is part of an oxidative stress sensing mechanism, promoting relocalization of DJ-1 from the cytosol to the outer mitochondrial membrane (*18*, *21*). In addition, DJ-1 has been shown to prevent the fibrillization of α-synuclein via a redox-dependent chaperone activity (*23*, *24*). Together, these observations suggest that a loss of DJ-1 function may induce nigral degeneration by disrupting the protein's antioxidant and/or chaperone function(s).

The X-ray structure of wild-type DJ-1 indicates that the protein exists as a homodimer of ∼20 kDa subunits with an α/*β* fold (*25*−*29*). Additional evidence in support of a dimeric structure has been obtained by gel-filtration analysis of the recombinant protein (*29*, *30*), coimmunoprecipitation of epitope-tagged subunits (*30*−*32*), and yeast two-hybrid studies (*32*, *33*). Residues at the subunit interface are highly conserved among various species, implying that DJ-1 must form a homodimer to carry out its biological function (*25*−*29*). Consistent with this idea, the crystal structure of DJ-1 suggests that dimer formation is necessary for the assembly of two symmetry-related active sites for cysteine 106 oxidation, each comprising residues from both subunits (*28*). One of the familial mutants, L166P, has a pronounced dimerization defect, resulting in decreased stability and failure of the protein to accumulate in eukaryotic cells (*21*, *30*−*32*). L166P also forms high-order protein complexes in cell culture, presumably because of its inability to adopt a stable, dimeric structure (*34*, *35*). Although the structural properties of L166P are well characterized, other DJ-1 mutants linked to familial PD have been less extensively studied.

In addition to familial DJ-1 mutants, oxidatively modified forms of the wild-type protein may play a role in PD pathogenesis (*36*, *37*). A groundbreaking proteomic study showed that wild-type DJ-1 was oxidized to a greater extent in the brains of patients with sporadic PD than in age-matched controls (*36*). In addition, the oxidation of DJ-1 was shown to increase with age in flies, mice, and humans, and this enhanced oxidation correlated with decreased resistance to oxidative stress (*37*). These observations suggest that oxidation of wild-type DJ-1 during aging may elicit a loss of DJ-1 function, thereby contributing to the onset of sporadic PD. Presumably, oxidative modifications that disrupt DJ-1 function are more extensive than the discrete modifications involved in the protein's sensing mechanism (i.e., oxidation to sulfinic acid at C106). Consistent with this idea, a partially oxidized DJ-1 isoform in which cysteine 106 is converted to the sulfinic acid suppresses α-synuclein fibrillization, whereas over-oxidized forms of the protein have lost this chaperone function (*24*). Despite evidence suggesting that over-oxidation disrupts DJ-1 function, the details of how oxidation affects the structure and stability of DJ-1 are unclear.

We hypothesized that other familial mutations (in addition to L166P) and over-oxidation impair DJ-1 function by destabilizing the protein's structure. To address this hypothesis, we characterized variants of human, recombinant DJ-1 (wild-type, M26I, E64D, over-oxidized wild-type, and C106A) in terms of quaternary structure and thermodynamic stability. Our data indicate that the familial mutant M26I and the over-oxidized wild-type protein have decreased stability and an increased propensity to form high molecular weight oligomers compared to that of wild-type DJ-1 that has not been subjected to oxidative treatment. These results provide a structural rationale for DJ-1 dysfunction in familial and sporadic PD, and they imply that stabilization of the native dimer may be a useful therapeutic strategy to treat both forms of this disorder.

EXPERIMENTAL PROCEDURES

Preparation of Bacterial Expression Constructs. A cDNA encoding wild-type human DJ-1 with an N-terminal hexahistidine tag was amplified by PCR and subcloned as an Xba I−Hind III fragment into pT7-7, yielding the construct pT7-7-DJ-1. Constructs encoding three mutant forms of DJ-1, M26I, E64D, and C106A were produced using the Quikchange method (Stratagene). The sequence of the DJ-1-encoding insert in each construct was verified using an Applied Biosystems (ABI 3700) DNA sequencer (University of Wisconsin−Madison or Purdue University). The familial mutant L166P was not analyzed because it has been well characterized by other groups (*21*, *30*−*32*), and the yields of this variant in our *E. coli* expression system were low.

Purification of Recombinant Human DJ-1. Cells of the BL21(DE3) strain of *Escherichia coli* were transformed with each pT7-7-DJ-1 construct by electroporation. To prepare recombinant DJ-1, the cells were grown to an OD_{600} of 0.6−0.8 in LB plus ampicillin (100 *μ*g/mL) at 37 °C, and expression of the DJ-1 gene was induced by adding IPTG (1 mM). The cells were grown under inducing conditions for 4 h at 37 °C, harvested by centrifugation, resuspended in buffer L (10 mM Tris HCl at pH 8.0, 1 mM PMSF, and 15 mM 2ME), and lysed with a French pressure cell (psi > 1000) (Thermo Electron Corporation, Waltham, MA). After centrifugation, DJ-1 was partially purified from the supernatant by successive ammonium sulfate precipitations (70% saturation followed by 90% saturation, 0 °C). The pellet from the second ammonium sulfate precipitation was resuspended in buffer A (10 mM Tris HCl at pH 8.0, 500 mM NaCl, 10 mM imidazole, and 15 mM 2ME), and the protein solution was applied to an immobilized metal affinity column charged with $NiCl_2$. DJ-1 was eluted in buffer A supplemented with 500 mM imidazole. Fractions most highly enriched with DJ-1 were identified by SDS−PAGE with Coomassie Brilliant Blue staining and pooled. The purity of the final protein sample was estimated to be approximately 98%, and the yield was 20−40 mg/L of bacterial culture. The DJ-1 samples were supplemented with glycerol (5%, [v/v]) and DTT (3 mM), and aliquots were frozen at −80 °C. For all of the analyses outlined below (except sedimentation equilibrium), the concentration of recombinant DJ-1 was estimated using the BCA Protein Assay kit (Pierce) and verified by quantitative amino acid analysis (Purdue University Proteomics Core).

Although the DJ-1 constructs were designed so that the histidine tag could be removed by proteolysis at an enter-

Table 1: Subunit Association/Dissociation Parameters for DJ-1 Variants Analyzed by Sedimentation Equilibrium

protein	best-fit model	molecular weight[a]	K_d (M)[b]
wild-type DJ-1	monomer−dimer	$3.6 \pm 0.1 \times 10^4$	$5 \pm 1 \times 10^{-7}$
M26I	monomer−dimer−tetramer	$3.4 \pm 0.1 \times 10^4$	ND[c]
E64D	monomer−dimer	$3.85 \pm 0.04 \times 10^4$	$3.4 \pm 0.6 \times 10^{-8}$
C106A	dimer	$3.9 \pm 0.1 \times 10^4$	ND[d]
wild-type DJ-1 (over-oxidized)	monomer−dimer−tetramer	$2.9 \pm 0.4 \times 10^4$	ND[e]

[a] The data are presented as the average apparent molecular weight ± SD from 2 to 5 independent runs. [b] The results are presented as the K_d ± SD from a single run in which eight or nine data sets could be used for fitting to a monomer−dimer model. The SD was estimated by comparing the raw values from the multiple data sets within each run. [c] ND, not determined (due to the complexity of the monomer−dimer−tetramer model). Data from one ultracentrifugation run were best fit to a monomer−dimer equilibrium with an estimated K_d of $2.8 \pm 0.8 \times 10^{-7}$. [d] ND, not determined. (K_d cannot be deduced from a dimer best-fit model.) The second best fit was to a monomer−dimer equilibrium, from which we estimated a K_d value of 1.2×10^{-8} M. [e] ND, not determined (due to the complexity of the monomer−dimer-tetramer model). Data from one ultracentrifugation run were best fit to a monomer−dimer equilibrium with an estimated K_d of $3 \pm 2 \times 10^{-6}$ M.

okinase cleavage site, we found that the tag was removed very inefficiently and with very low yields. Accordingly, the studies outlined below were carried out with intact histidine-tagged DJ-1 variants. Two observations suggest that our approach was reasonable. First, data from another group indicate that untagged M26I is less stable than untagged wild-type DJ-1 in the presence of denaturant (Ray, S.S., unpublished observations), a result similar to that obtained with the corresponding histidine-tagged variants (see below). Second, the presence of an N-terminal histidine tag has no impact on the degree of neuroprotection by wild-type or mutant DJ-1 in a primary cell-culture model of PD (Liu et al., unpublished work).

Size-Exclusion Chromatography. Protein solutions (~1 mg/mL final concentration) were dialyzed against phosphate buffered saline (PBS, 10 mM phosphate buffer, 2.7 mM KCl, and 137 mM NaCl at pH 7.4), and an aliquot (125−250 μg) was applied to a Superdex 200 size-exclusion chromatography (SEC) column (GE Healthcare). The protein was eluted with PBS at a flow rate of 0.25 mL/min, monitoring absorbance at 280 nm. Apparent molecular weights of eluted proteins were determined using a calibration curve established with the following standards: Blue dextran (>600 kDa), BSA (66.2 kDa), ovalbumin (43 kDa), and lysozyme (14.3 kDa).

Sedimentation Equilibrium. Sedimentation-equilibrium runs were conducted at 22 °C in a Beckman XL-I analytical ultracentrifuge (Beckman Coulter, Fullerton, CA) using absorbance optics, as described by Laue and Stafford (*38*). Prior to ultracentrifugation, protein samples were dialyzed against 50 mM Tris at pH 7.0 and 200 mM NaCl (4 °C, 48 h, with a change in buffer after 24 h). Aliquots (110 μL) of the protein solution (0.7−2.5 mg/mL) were loaded into six-sector CFE sample cells, allowing three concentrations to be run simultaneously. Runs were performed at a minimum of three different speeds (2.0×10^4−2.4×10^4 rpm), and each speed was maintained until there was no significant difference in scans of $r^2/2$ versus absorbance taken 2 h apart to ensure that equilibrium was achieved. Sedimentation-equilibrium data were evaluated using the program NONLIN, which employs a nonlinear least-squares curve-fitting algorithm described by Johnson et al. (*39*). The program allows for analysis of both single and multiple data files and can be fit to models containing up to four associating species, depending upon which parameters are permitted to vary during the fitting routine. The protein's partial specific volume and the solvent density were estimated using the Sednterp program (*40*). Between two and five independent ultracentrifugation runs were carried out for each DJ-1 variant. The average apparent molecular weights presented in Table 1 were calculated from the individual molecular weights determined from separate runs. Although a value for the dimer dissociation constant (K_d) can be obtained from sedimentation data that are best fit to a monomer−dimer equilibrium, in practice we find that a reliable K_d value is only determined from runs in which eight or nine data sets can be used for the fitting. Only one run with ≥8 usable data sets was obtained for wild-type DJ-1 and E64D. The K_d values from these individual best-fit runs are presented in Table 1.

Protein Cross-Linking. Variants of DJ-1 (10 μL, 0.2 mg/mL) were dialyzed against 25 mM potassium phosphate (KP_i) at pH 7.4 and 150 mM NaCl and treated with DMF (vehicle control) or the primary amine cross-linker DSS (4 mM). The samples were analyzed by SDS−PAGE using a 4−20% polyacrylamide gel. After staining with Coomassie Brilliant Blue, bands on the gel were quantified by measuring average pixel intensities using a Typhoon Imaging System. For each DJ-1 isoform, the signal corresponding to the cross-linked dimer was normalized to the monomer signal in the sample treated with DMF.

Thermal Denaturation. Protein solutions were dialyzed against 10 mM KP_i at pH 7.0 and 150 mM NaCl. Aliquots of the protein (125 μL, 1 mg/mL) were incubated at 22 or 42 °C for 1 h and analyzed by SEC using a Superdex 200 column, as described above. In parallel experiments, aliquots of the protein (0.4 mL, 3 μM) were introduced into a 0.2 cm quartz cuvette and analyzed by far-UV CD using a J810 spectropolarimeter (JASCO, Easton, MD), at temperatures ranging from 20 to 80 °C (temperature ramp rate, 5.0 °C/min). The ellipticity at 220 nm was recorded at increments of 1 °C. Full spectra were collected at 20 °C with a bandwidth of 2 nm, a response time of 1 s, and a data pitch of 1 nm. Molar ellipticity was calculated using the following equation:

$$[\theta]_\lambda = \frac{m \cdot \theta_\lambda}{10 \cdot d \cdot c}$$

where $[\theta]_\lambda$ is the molar ellipticity, m is the mean residual weight (g/mol), θ_λ is the ellipticity, d is the path length (cm), and c is the protein concentration (g/L).

Urea Denaturation. Protein solutions were dialyzed against 50 mM KP_i at pH 7.0 and 1 mM 2ME. Alternatively, proteins

treated with H_2O_2 (see below) were eluted in 50 mM KP_i (without 2ME) from a HiPrep 26/10 desalting column. After dialysis or desalting, the protein concentration was determined using the BCA Protein Assay kit. An aliquot of the protein (final concentration 3 or 12 μM) was treated overnight with 0−6 M urea at 22 °C. (The solutions were prepared using a stock solution of 10 M urea in the dialysis buffer.) Each protein sample was analyzed by far-UV CD as described above. Spectra were recorded using the same instrument parameters (bandwidth, response time, and data pitch) as outlined above.

Calculation of the Apparent Free Energy of Unfolding in the Absence of Denaturant. To facilitate the numerical analyses of thermodynamic parameters, a reversible two-state transition between native dimeric DJ-1 and unfolded monomer was assumed throughout these studies (*41*−*45*). Values of $[\Delta G_u^{H_2O}]_{app}$ were estimated by fitting the data to the following equations (*46*, *47*):

$$y = f_u\,(y_u + ds[\text{urea}]) + (1 - f_u)(y_n + ns[\text{urea}])$$

$$f_u = \{-K_{d,app} + ([K_{d,app}]^2 + 8P_t\,K_{d,app})^{0.5}\}/(4P_t)$$

$$K_{d,app} = \exp\{(-[\Delta G_u^{H_2O}]_{app} + m[\text{urea}])/RT\}$$

where y is the observed ellipticity ($[\theta]_{obs}$) at a given concentration of urea; y_n and y_u are the extrapolated ordinate intercept values of $[\theta]_{obs}$ for the native and unfolded protein, respectively; *ns* and *ds* are the slopes of the baselines for the native and denatured protein, respectively; f_u is the molar fraction of unfolded protein; $K_{d,app}$ is the apparent equilibrium dissociation constant; R is the universal gas constant (0.001986 kcal/mol·K); T is the absolute temperature (K); m is a constant proportional to the increase in the solvent-accessible surface area of the protein upon denaturation (*48*); and P_t is the total concentration of monomeric protein in M. Values of $[\text{urea}]_{1/2}$ were estimated by fitting the data to the equations listed above, substituting $[\Delta G_u^{H_2O}]_{app}$ with the following expression (*49*):

$$[\Delta G_u^{H_2O}]_{app} = m[urea]_{1/2} - RT\ln P_t$$

The data were fitted using the program TableCurve 2D (Jandel Scientific, San Rafael, CA), with r^2 values of 0.99 or greater. Errors are reported as the standard errors given by the program.

Over-Oxidation of DJ-1. To determine the effects of over-oxidation on the structure and stability of DJ-1, aliquots of the purified protein were dialyzed against 10 mM Tris at pH 8.0 to remove reductant, and the protein was treated with a 10-fold molar excess of H_2O_2 for 1 h at 22 °C. Excess H_2O_2 was removed from each sample by exchanging the protein into fresh buffer via elution from a HiPrep 26/10 desalting column. The protein was eluted in (i) 10 mM KP_i at pH 7.0 and 150 mM NaCl prior to thermal denaturation analysis by far-UV CD; (ii) 50 mM KP_i at pH 7.0 prior to urea denaturation; or (iii) 10 mM Tris at pH 8.0 prior to sedimentation analysis.

Isoelectric Focusing. To determine relative differences in the abundance of isoforms with different pI values, recombinant wild-type or mutant DJ-1 was dialyzed against 10 mM Tris at pH 8.0, and an aliquot (9 μg) was loaded onto an isoelectric focusing (IEF) gel with a pH range of 3−7 (Invitrogen). Samples were run at the following voltages in sequence: 100 V for 1 h, 200 V for 1 h, and 300 V for 1 h. The separated protein isoforms were imaged by silver staining, and approximate pI values were determined by comparison with IEF standards (Bio-Rad).

Proteolysis and Mass Spectrometry. Recombinant DJ-1 was precipitated with ice-cold trichloroacetic acid (10%, w/v), and the pellet was washed with ethyl acetate/ethanol (50:50, v/v) and dried. The protein was trypsinized and prepared for analysis via liquid chromatography-tandem mass spectrometry (LC-MS/MS) as described previously (*50*). The digested, desalted protein samples were analyzed using a Sciex QSTAR hybrid LC-MS/MS Quadrupole time-of-flight mass spectrometer. All spectra were obtained in the positive ion mode using nanospray ionization. Peptides identified in each sample were sequenced in MS/MS mode. The sequences of the peptides were determined by subjecting the MS/MS results to a database search using the program Mascot (*51*). A Mascot cutoff score of 15 was used in these studies (typical range of Mascot scores for a given dataset: 15−80).

RESULTS

Quaternary Structure and Stability of Wild-Type and Mutant DJ-1. In the first part of our study, we assessed the relative dimerization propensity of wild-type DJ-1, M26I, and E64D via SEC using a Superdex 200 column. The wild-type protein eluted as a single major species with an apparent molecular weight equal to that of dimeric DJ-1 (Figure 1A). In contrast, SEC data obtained for M26I indicated that this variant consisted of high-molecular weight species, including oligomers eluted in the column void volume (>600 kDa), and a species with an apparent molecular weight of 54 kDa (Figure 1B). The fact that the apparent molecular weight of the 54 kDa species was greater than that of the wild-type dimer suggested that M26I was partially unfolded and/or existed as a mixture of rapidly equilibrating oligomers (e.g., dimer and trimer), in addition to higher-order aggregates. In contrast to M26I, E64D eluted as a single peak similar to the elution of the wild-type dimer (Figure 1C).

In parallel with SEC, we analyzed the quaternary structure of wild-type and mutant DJ-1 via ultracentrifugation. The data obtained for wild-type DJ-1 were best fit to a monomer−dimer model with an estimated K_d of $5 \pm 1 \times 10^{-7}$ M (Figure 2A; Table 1). In contrast, sedimentation-equilibrium data from multiple analyses of M26I were best fit to a monomer−dimer−tetramer model (Figure 2B; Table 1). Data from one analysis of M26I were best fit to a monomer−dimer equilibrium with an estimated K_d of $2.8 \pm 0.8 \times 10^{-7}$ M. The data obtained for E64D were best fit to a monomer−dimer model, with an estimated K_d 1 order of magnitude less than that obtained for wild-type DJ-1 (Figure 2C; Table 1).

Quaternary structural analyses of wild-type and mutant DJ-1 were also conducted via chemical cross-linking followed by SDS−PAGE. After treatment with the cross-linker DSS, wild-type DJ-1 consisted of three major electrophoretic species, apparently corresponding to the cross-linked dimer, uncross-linked monomer, and intramolecularly cross-linked monomer (Figure 3A). In contrast, M26I treated with DSS

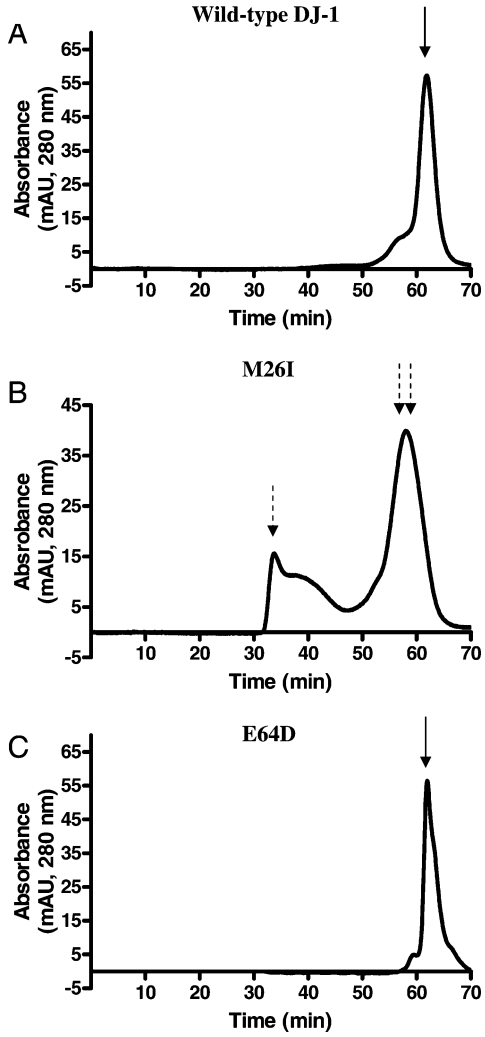

FIGURE 1: M26I forms high molecular weight aggregates to a greater extent than wild-type DJ-1 or E64D. Wild-type DJ-1 (A), M26I (B), or E64D (C) (250 μL, 1 mg/mL) was injected on a Superdex 200 (10/30) column and eluted with PBS at a flow rate of 0.25 mL/min. Solid arrow: species with an apparent molecular weight of 43 kDa (dimer); dashed arrow: void-volume oligomer (>600 kDa); double dashed arrow: species with an apparent molecular weight of 54 kDa (altered dimer).

migrated primarily as a smear on the gel, most likely corresponding to a heterogeneous mixture of cross-linked oligomers, whereas the relative amount of cross-linked dimer was significantly lower than that in the sample of wild-type DJ-1 (Figure 3A and B). E64D exhibited a similar pattern of cross-linked species as the wild-type protein (Figure 3A and B).

Next, wild-type and mutant DJ-1 were characterized in terms of secondary structure and thermodynamic stability by far-UV CD. Spectra recorded for the wild-type protein and E64D displayed broad negative ellipticity from 208 to 222 nm (Figure 4A), consistent with a mixed α/β structure. In contrast, the M26I spectrum exhibited an overall reduction in negative ellipticity from 208 to 222 nm, suggesting that M26I had reduced secondary structure (Figure 4A). We also assessed the stability of wild-type and M26I DJ-1 by monitoring thermal denaturation. Wild-type DJ-1 and E64D (3 μM) exhibited similar cooperative unfolding transitions with average T_m values of 66.1 and 64.5 °C, respectively (Figure 4B). Both variants recovered approximately 65% of their initial ellipticity at 220 nm upon cooling from 80 to 20 °C, albeit with some hysteresis (Figure 4C). These findings suggested that the thermal unfolding of wild-type DJ-1 and E64D was largely reversible (*52*). In contrast, M26I had reduced absolute ellipticity that did not change with increasing temperature (Figure 4B). Because M26I did not undergo a cooperative unfolding transition, we were not able to calculate a T_m for this variant.

To address whether M26I has a higher propensity to form heat-induced aggregates compared to that of wild-type DJ-1 or E64D, each protein was analyzed by SEC after incubation at 42 °C for 1 h. A heated sample of wild-type DJ-1 eluted primarily as the native dimer, along with a minor fraction of oligomeric species (Figure 4D). E64D remained fully dimeric after heating, forming no detectable oligomer (Figure 4D). In contrast to wild-type DJ-1 and E64D, heated M26I consisted mostly of high molecular weight oligomers, and the level of dimer was substantially lower than in the untreated sample (compare Figure 4D to Figure 1B). These data indicated that M26I underwent aggregation more readily than wild-type DJ-1 or E64D at elevated temperatures. Preincubation at 22 °C for 1 h had no effect on the chromatographic profiles of any of the DJ-1 variants compared to untreated controls (results similar to Figure 1A−C, data not shown).

To further explore the stability differences among wild-type DJ-1, M26I, and E64D, we monitored the unfolding of the proteins in the presence of chaotrope. Wild-type DJ-1 (12 μM) exhibited a cooperative unfolding transition, with a $[\Delta G_u^{H_2O}]_{app}$ of 10.4 ± 0.3 kcal mol^{-1} and an unfolding midpoint ($[urea]_{1/2}$) of 1.95 M urea (Figure 4E; Table 2). A comparison of unfolding and refolding curves indicated that wild-type DJ-1 recovered much of its initial ellipticity upon refolding, albeit with some hysteresis (data not shown). This observation suggested that the urea-induced unfolding of wild-type DJ-1 was mostly reversible (*52*). In contrast, M26I did not exhibit a cooperative unfolding transition with a folded state baseline. Rather, the absolute ellipticity of this mutant was markedly lower at 0 M urea and decreased gradually upon the addition of denaturant (Figure 4E). E64D exhibited a cooperative unfolding transition similar to that of wild-type DJ-1, with slightly reduced values for $[\Delta G_u^{H_2O}]_{app}$ and $[urea]_{1/2}$ (Figure 4E; Table 2)

From all of these results, we inferred that M26I has reduced secondary structure, decreased stability, and a higher propensity to aggregate compared to that of wild-type DJ-1. In contrast, E64D is similar to the wild-type protein in terms of secondary structure and thermodynamic stability.

Quaternary Structure and Stability of Over-Oxidized Wild-Type DJ-1. To address whether excess oxidation causes a reduction in the stability of DJ-1, we examined the quaternary structure and stability of the wild-type protein after exposure to oxidizing conditions. The wild-type protein was incubated with a 10-fold molar excess of H_2O_2 for 1 h at 22 °C, a treatment shown previously to cause oxidation of DJ-1 (*10*, *24*). We refer to protein subjected to this treatment as over-oxidized because IEF and mass spectrometry data suggested that all of our DJ-1 variants were partially oxidized, even prior to incubation with H_2O_2 (see below). Sedimentation-equilibrium data from multiple analyses of the peroxide-treated protein were best fit to a monomer−dimer−tetramer model (Table 1). Data from one run were best fit to a

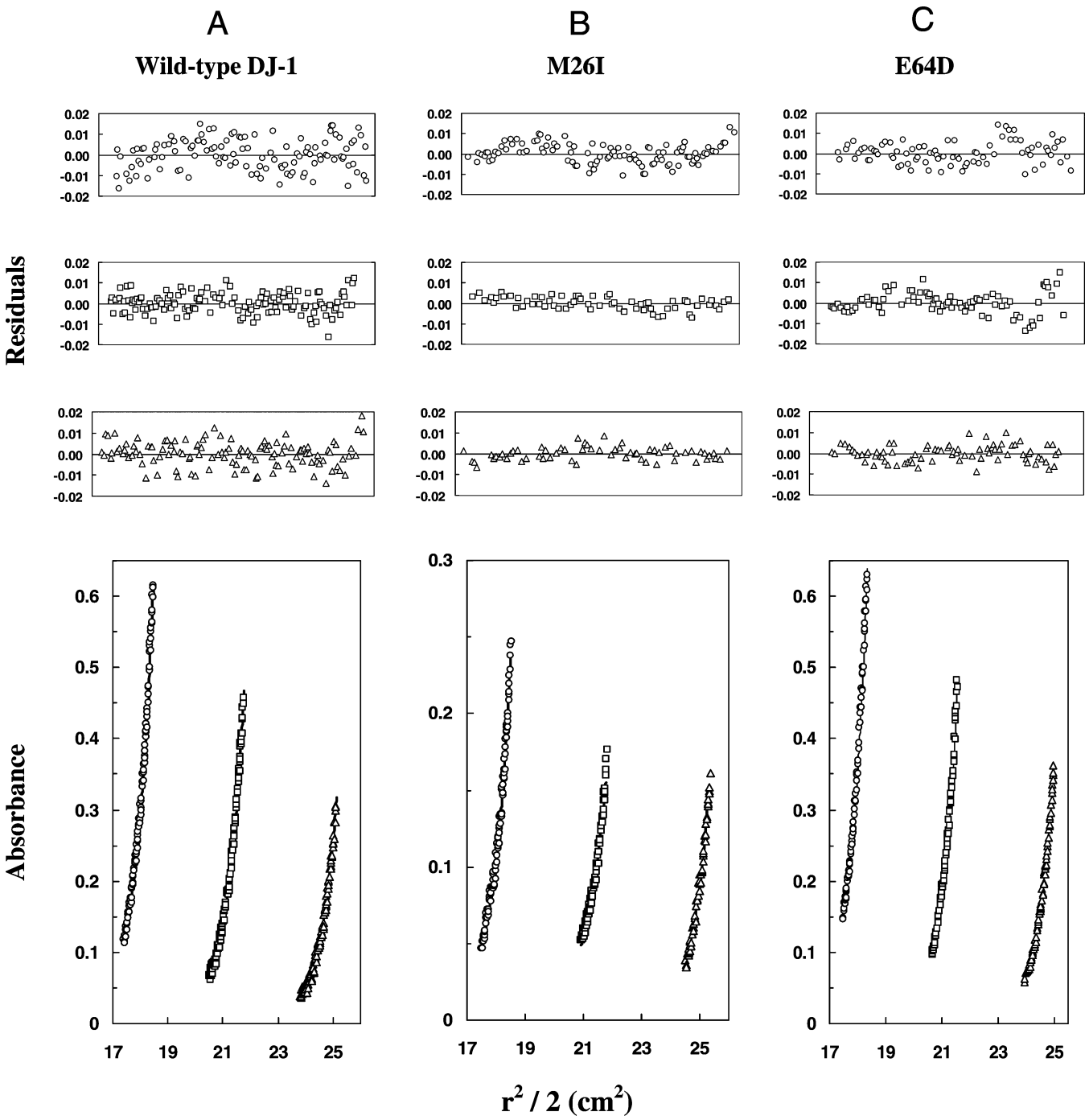

FIGURE 2: Sedimentation-equilibrium analysis of wild-type and mutant DJ-1. Wild-type DJ-1, M26I, or E64D was centrifuged at 20000, 22000, and 24000 rpm at 22 °C. (Only the data collected at 20000 rpm are shown.) The protein concentration was 2.20 mg/mL (○), 1.47 mg/mL (□), or 1.10 mg/mL (△) for wild-type DJ-1 (A); 1.42 mg/mL (○), 0.95 mg/mL (□), or 0.71 mg/mL (△) for M26I (B); and 2.29 mg/mL (○), 1.67 mg/mL (□), or 1.25 mg/mL (△) for E64D (C). The lower graphs illustrate plots of $r^2/2$ versus absorbance. The symbols represent measured data points, and the solid lines represent best-fit curves to a monomer−dimer model (A and C) or a monomer−dimer-tetramer model (B). The upper graphs illustrate the residuals from the fitting. The random, nonsystematic distribution of the residuals indicates a good fit of the data to the models.

monomer−dimer equilibrium with a significantly greater K_d value than that obtained for untreated, wild-type DJ-1 (Table 1). SEC analysis showed that the over-oxidized protein had a tendency to form oligomeric species that were absent from samples of untreated wild-type DJ-1, although the extent of aggregation was variable (data not shown). Far-UV CD analysis revealed an overall reduction in negative ellipticity from 208 to 222 nm compared to that of the untreated, wild-type protein (Figure 5A). Over-oxidized DJ-1 also underwent a less cooperative unfolding transition at elevated temperatures (Figure 5B). From these data, we inferred that wild-type DJ-1 converts to a form with a tendency to aggregate under conditions of oxidative stress, perhaps due to partial destabilization of the native dimer.

Effect of Oxidation on M26I and E64D Stability. Because wild-type DJ-1 was destabilized by over-oxidation, we reasoned that the relative stabilities of wild-type and mutant DJ-1 observed earlier in this study might reflect differences in oxidation during expression in *E. coli* and purification. To address this hypothesis, we analyzed wild-type DJ-1,

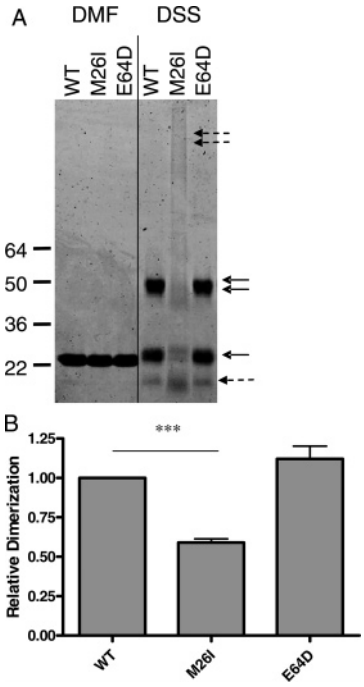

FIGURE 3: M26I has a decreased dimerization propensity compared to that of wild-type DJ-1 or E64D. (A) Extent of dimerization monitored by chemical cross-linking. Wild-type DJ-1 (WT), M26I, or E64D (10 μL, 0.2 mg/mL) was treated with DMF (vehicle control) or the primary amine cross-linker DSS and analyzed by electrophoresis on a 4−20% SDS−PAGE gel with Coomassie Blue staining. Double dashed arrow: SDS-resistant DJ-1 aggregates; double solid arrow: dimeric DJ-1; single solid arrow: monomeric DJ-1; single dashed arrow: intramolecularly cross-linked monomer. Molecular weight markers are shown to the left of the gel. (B) Quantification of the extent of dimerization. For each DJ-1 variant, relative dimerization was determined by dividing the chemifluorescent signal for the cross-linked dimer (DSS lanes) by the signal for the uncross-linked monomer (DMF lanes). The data are plotted as the amount relative to the wild-type dimer level (mean ± SEM, $N = 3$, ***$P < 0.001$, WT vs M26I, ANOVA with Newman−Keuls post test).

M26I, and E64D via IEF. All three proteins (not treated with H_2O_2) consisted of similar distributions of isoforms with pI values ranging from 6.0 to 6.5 (Figure 6). Although these results indicated that a portion of each protein was already oxidized during expression and purification, we inferred that the stability differences observed previously were not due to striking differences in the extent of oxidation *per se*. However, M26I exhibited an overall decrease in the relative abundance of the most acidic isoforms (pI range ~6.0−6.1), and this decrease correlated with the appearance of insoluble material near the top of the gel (Figure 6). These data implied that some acidic (oxidized) isoforms of M26I may have a high propensity to form high molecular weight aggregates.

In parallel with the IEF analysis, oxidative modifications of wild-type DJ-1, M26I, and E64D were characterized by LC-MS/MS. Data obtained for representative samples are shown in Table 3. The results indicated that all three variants were partially oxidized to cysteine sulfinic acid (2O) or cysteine sulfonic acid (3O) at position 106, even without exposure to H_2O_2. Other modifications identified by LC-MS/MS included methionine sulfoxide (at two different sites on wild-type DJ-1 and M26I) and cysteine sulfonic acid (at positions 46 and 53 of wild-type DJ-1) (Table 3). These results confirmed that wild-type DJ-1, M26I, and E64D were oxidized during expression and purification. Moreover, the data supported our earlier conclusion that stability differences among the three variants were not due to pronounced differences in the degree of oxidation.

Quaternary Structure and Stability of C106A. Although oxidation of cysteine 106 to the sulfinic acid is thought to be essential for the antioxidant and chaperone functions of DJ-1 (*18*, *24*), it has been suggested that further oxidation at this site may inactivate the protein (*24*, *37*). We hypothesized that over-oxidation of cysteine 106 might be partly responsible for the destabilization and aggregation of wild-type DJ-1 under oxidizing conditions. To address this hypothesis, we characterized the quaternary structure and stability of the engineered mutant, C106A. As this variant is unable to undergo oxidation at position 106, we predicted that it would be less susceptible to destabilization upon exposure to H_2O_2 than wild-type DJ-1. Moreover, because recombinant DJ-1 undergoes oxidation at position 106 during expression and purification (Table 3), we speculated that C106A might be more stable than the wild-type protein even in the absence of peroxide treatment. IEF analysis revealed that untreated C106A consisted of fewer acidic isoforms than wild-type DJ-1 (Figure 7A). LC-MS/MS data indicated that the mutant had a profile of modifications similar to that of the wild-type protein except for the absence of oxidation at position 106, as expected (Table 3). SEC analysis of untreated C106A revealed a single peak corresponding to the native dimer (Figure 7B). In addition, sedimentation-equilibrium data obtained for the untreated mutant were best fit to a dimer model (Table 1). Although a K_d value cannot be deduced from this model, the second best fit for these data was to a monomer−dimer equilibrium, and in this case the estimated K_d value was 1.22×10^{-8} M. Upon cross-linking with DSS, untreated C106A showed a distribution of species nearly identical to that of the wild-type protein, with no evidence of higher order oligomers (Figure 7C and D). The SEC elution profile of C106A was unchanged after treating the mutant with a 10-fold molar excess of H_2O_2 (data not shown).

Next, we characterized the C106A mutant in terms of secondary structure and thermodynamic stability. Far-UV CD analysis of untreated C106A revealed a spectrum with broad negative ellipticity from 208 to 222 nm, similar to the spectra obtained for wild-type DJ-1 and E64D (Figure 8A). The untreated mutant also had a greater thermal stability (Figure 8B) and a decreased propensity to form high molecular weight oligomers at high-temperature (Figure 8C) compared to wild-type DJ-1. Untreated C106A exhibited a cooperative unfolding transition in urea with a midpoint ($[urea]_{1/2}$) greater than that observed for the wild-type protein (Figure 8D; Table 2). The value of $[G_u^{H_2O}]_{app}$ calculated assuming a reversible two-state transition was also substantially greater for C106A than for wild-type DJ-1 (Table 2). The secondary structure and stability of C106A were unaffected by treatment of the protein with excess H_2O_2 (Figure 8A, B, and D).

From these data, we inferred that the stability of C106A is greater than that of wild-type DJ-1 and is unchanged by oxidation. In turn, these findings suggest that the loss of secondary structure and reduced stability of over-oxidized wild-type DJ-1 result in part from the oxidation of C106.

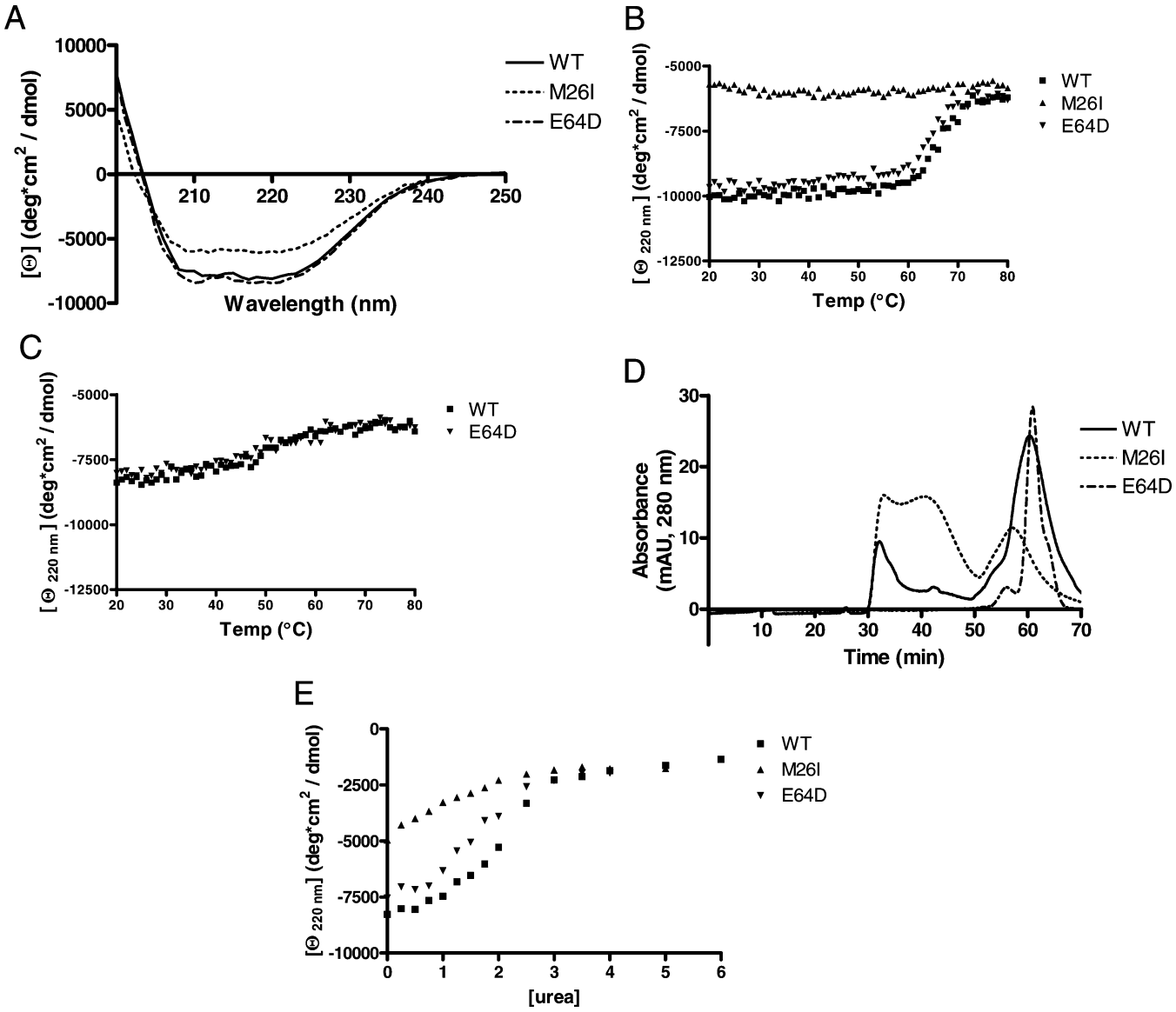

FIGURE 4: M26I has decreased secondary structure and reduced thermodynamic stability compared to that of wild-type DJ-1 and E64D. (A) Secondary structure of wild-type or mutant DJ-1 (12 μM) determined by far-UV CD. (B) Thermal unfolding of wild-type or mutant DJ-1 (3 μM) monitored by far-UV CD. Ellipticity was measured at 220 nm with heating at a rate of 5 °C/min over a range of 20−80 °C. (C) Refolding of wild-type DJ-1 or E64D (3 μM) monitored by far-UV CD. Ellipticity was measured at 220 nm with cooling at a rate of 5 °C /min over a range of 80−20 °C. (D) Heat-induced unfolding and aggregation monitored by SEC. Wild-type or mutant DJ-1 (125 μL, 1 mg/mL) was incubated at 42 °C for 1 h and eluted from a Superdex 200 (10/30) column with PBS at a flow rate of 0.25 mL/min. (E) Urea-induced unfolding monitored by far-UV CD. Wild-type DJ-1, M26I, or E64D (12 μM) was incubated overnight at room temperature in phosphate buffer containing various amounts of urea (0−6 M), and ellipticity was measured at 220 nm.

Table 2: Equilibrium Unfolding Parameters for DJ-1 Variants Denatured with Urea

protein	P_t (μM)	$[\Delta G_u^{H_2O}]_{app}$ (kcal mol^{-1})	m (kcal mol^{-1} M^{-1})	$[urea]_{1/2}$ (M)
wild-type DJ-1	12	10.4 ± 0.3	1.9 ± 0.2	1.95 ± 0.05
E64D	12	9.2 ± 0.5	1.8 ± 0.3	1.42 ± 0.08
wild-type DJ-1	3	9.1 ± 0.4	1.9 ± 0.3	0.81 ± 0.09
C106A (untreated)	3	25 ± 5	5 ± 1	3.41 ± 0.05
C106A (over-oxidized)	3	22 ± 2	4.3 ± 0.5	3.31 ± 0.03

DISCUSSION

In this article, we characterized several variants of recombinant human DJ-1 (wild-type, M26I, E64D, over-oxidized wild-type, and C106A) in terms of quaternary structure, secondary structure, and thermodynamic stability. An advantage of examining recombinant DJ-1, as we have done here, is that a test tube model is an isolated system so that the data from these studies provides insight into the intrinsic structural defects of DJ-1 that may account for its loss of function in familial or sporadic PD. Additionally, our protein preparations exhibited an oxidation pattern similar to that of DJ-1 from the brains of PD patients (*36*), suggesting that the biochemical and biophysical properties of recombinant DJ-1 may be relevant to the pathogenesis of PD.

M26I and E64D Substitutions Have Different Effects on the Stability and Structure of DJ-1. Our data confirm previous findings that recombinant wild-type DJ-1 exists as a stable dimer with a low propensity to form higher-order oligomers (*29*, *30*). In contrast, M26I readily forms oligomers or aggregates, and this effect is even more pronounced at high temperatures. This high aggregation propensity of M26I

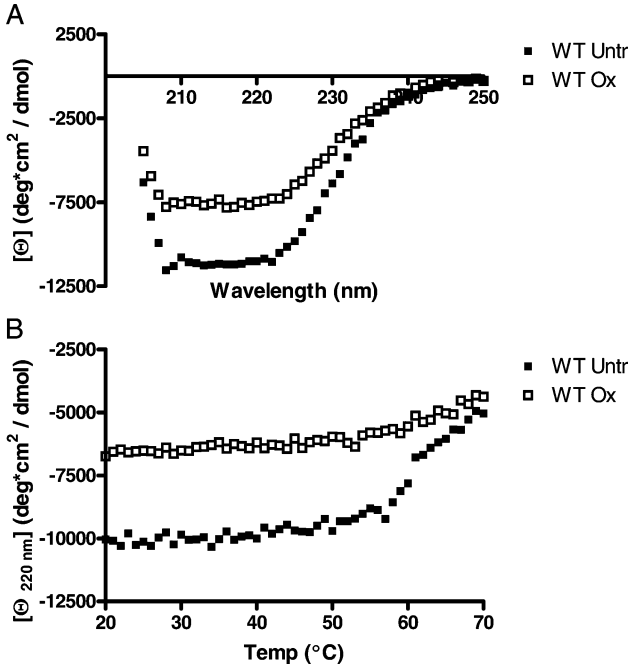

FIGURE 5: Over-oxidized wild-type DJ-1 has decreased secondary structure and reduced thermodynamic stability compared to untreated wild-type DJ-1. (A) Secondary-structure of untreated or over-oxidized wild-type DJ-1 (3 μM) determined by far-UV CD. (B) Thermal unfolding of untreated or over-oxidized wild-type DJ-1 (3 μM) monitored by far-UV CD. Ellipticity was measured at 220 nm with heating at a rate of 5 °C/min over a range of 20−70 °C.

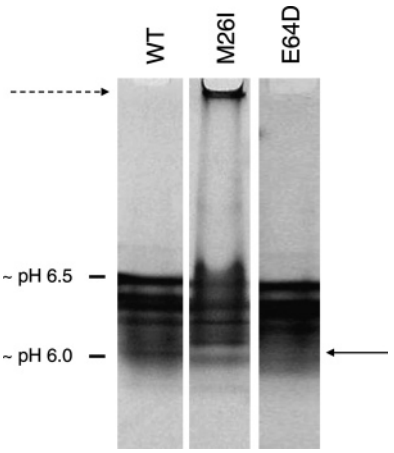

FIGURE 6: Wild-type and mutant DJ-1 consist of similar distributions of charged species. Untreated wild-type DJ-1, M26I, and E64D (9 μg of each) were loaded on a native IEF gel (pH range 3−7), and charged species were separated according to their pI values. The pI values of IEF standards are shown to the left of the gel. Each DJ-1 variant consisted of multiple isoforms with pI values spanning 6.0−6.5. The dashed arrow (top of the gel) indicates a band presumably corresponding to aggregated M26I. The solid arrow (lower right of the gel) indicates a zone with lower amounts of M26I compared to that of wild-type DJ-1 or E64D.

reflects an altered conformation of the mutant protein compared to that of wild-type DJ-1, as suggested by (i) the reduced absolute ellipticity observed for M26I, which may reflect a net conversion of α-helix to β-sheet (*53*, *54*); (ii) the anomalous elution time of dimeric M26I from an SEC column; and (iii) the failure of M26I to undergo cooperative unfolding in the presence of urea or at high temperatures. We also show through quantitative thermodynamic analyses that the M26I homodimer is less stable than the wild-type dimer. Our results are consistent with reports that M26I has reduced stability in cell-culture models (*21*, *32*) and that steady-state levels of M26I are increased in neuroblastoma cells treated with proteasome inhibitor (*31*). In contrast to our results from studies of recombinant M26I, cross-linking data obtained by two groups suggest that M26I does not exhibit a pronounced homodimerization defect in cell culture (*21*, *35*). This discrepancy may be due to the fact that the cross-linking data were obtained in cells expressing endogenous, wild-type DJ-1 and, therefore, reported on the formation of wild-type/M26I heterodimers in addition to homodimers. Heterodimer formation between M26I and WT may help stabilize the mutant protein, and this effect could play an important role in preserving DJ-1 function in heterozygous individuals.

Residue M26 is strictly conserved across all vertebrates, suggesting that it is critical for the structure and function of DJ-1 (*55*). The crystal structure of wild-type DJ-1 reveals that M26 is located on the C-terminal end of α-helix A, at the dimer interface (*25*−*29*). This α-helix is thought to promote dimerization by engaging in hydrophobic contacts with α-helix A from the opposite subunit (*28*). Accordingly, the M26I substitution may weaken the dimer by perturbing this interaction between α-helices at the subunit interface. Consistent with this idea, comparison of the predicted secondary structures of wild-type DJ-1 and M26I suggests that the M26I substitution promotes the conversion of α-helix A to a β-strand conformation (Figure S1, Supporting Information), a prediction supported by our far-UV CD data (see above). A structural perturbation in this region could unmask nearby hydrophobic residues including M17, V20, I21, and V23, and the exposure of these residues could in turn promote the aggregation of M26I (*28*).

Evidence from the wild-type DJ-1 crystal structure suggests that the M26I substitution may be especially destabilizing when the mutant protein is oxidized at C106. Two residues in the vicinity of M26, D24 and R28, are proposed to play a key role in stabilizing the sulfinic acid form of cysteine 106 by forming hydrogen bonds with the sulfinic oxygens (*28*). The M26I substitution may disrupt the protein conformation in this region and, consequently, perturb the hydrogen-bonding network. Our IEF and LC-MS/MS data indicate that recombinant wild-type DJ-1, M26I, and E64D are all partially oxidized at C106. In addition, the IEF data imply that oxidized isoforms of M26I have a high propensity to undergo misfolding and aggregation. Accordingly, a large part of the observed decrease in stability of M26I relative to wild-type DJ-1 may be due to destabilization of the oxidized protein by the M26I substitution. Moreover, cell-culture data indicate that M26I undergoes a more pronounced, oxidation-dependent relocalization to mitochondria (*21*), suggesting that the mutant is partially unfolded and more susceptible to oxidation than the wild-type protein.

Our data indicate that E64D and wild-type DJ-1 both form a stable dimer with nearly identical secondary structure and cooperative unfolding transitions. Two observations suggest that E64D may form a dimer with *increased* stability: (i) the K_d of E64D determined by sedimentation-equilibrium was approximately 10-fold lower than the corresponding value obtained for wild-type DJ-1; and (ii) E64D was less prone to aggregation upon extended incubation at elevated tem-

Table 3: Mass Spectral Data for Oxidized Peptides Derived from Wild-Type and Mutant DJ-1

DJ-1 variant	peptide sequence[a]	predicted mass for native DJ-1 (Da)	observed *m/z* (Da)	predicted modification
WT	^{13}GAEE**M**ETVIPVDV**M**RR^{28}	1830.90	$(924.44)^{2+}$	1 met sulfoxide
	^{39}AGKDPVQ**C**SRDVVI**C**PDASL^{58}	2072.00	$(1085.10)^{2+}$ $(723.73)^{3+}$ $(543.05)^{4+}$	2 cys sulfonic acid
	^{100}GLIAAI**C**AGPTALLAHEIGFGSK^{122}	2209.19	$(1121.60)^{2+}$	1 cys sulfinic acid
	^{131}DK**MM**NGGHYTYSENR^{145}	1801.75	$(909.86)^{2+}$ $(606.92)^{3+}$	1 met sulfoxide
	^{133}**MM**NGGHYTYSENR^{145}	1558.63	$(788.30)^{2+}$	1 met sulfoxide
M26I	^{13}GAEE**M**ETVIPVDVIRR^{28}	1812.94	$(610.67)^{3+}$	1 met sulfoxide
	^{99}KGLIAAI**C**AGPTALLAHEIGFGSK^{122}	2337.29	$(796.12)^{3+}$	1 cys sulfonic acid
	^{100}GLIAAI**C**AGPTALLAHEIGFGSK^{122}	2209.19	$(1121.64)^{2+}$ $(748.09)^{3+}$	1 cys sulfinic acid
	^{133}**MM**NGGHYTYSENR^{145}	1558.63	$(788.35)^{2+}$	1 met sulfoxide
E64D	^{99}KLIAAI**C**AGPTALLAHEIGFGSK^{122}	2337.29	$(1186.04)^{2+}$	1 cys sulfinic acid
	^{99}KLIAAI**C**AGPTALLAHEIGFGSK^{122}	2337.29	$(796.10)^{3+}$	1 cys sulfonic acid
	^{100}GLIAAI**C**AGPTALLAHEIGFGSK^{122}	2209.19	$(1121.64)^{2+}$	1 cys sulfinic acid
	^{100}GLIAAI**C**AGPTALLAHEIGFGSK^{122}	2209.19	$(1129.30)^{2+}$	1 cys sulfonic acid
C106A	^{13}GAEE**M**ETVIPVDV**M**R^{27}	1674.80	$(854.38)^{2+}$	2 met sulfoxide
	^{13}GAEE**M**ETVIPVDV**M**R^{27}	1674.80	$(564.60)^{3+}$	1 met sulfoxide
	^{13}GAEE**M**ETVIPVDV**M**RR^{28}	1830.90	$(616.62)^{3+}$	1 met sulfoxide
	^{33}VTVAGLAGKDPVQ**C**SR^{48}	1599.84	$(824.88)^{2+}$	1 cys sulfonic acid
	^{131}DK**MM**NGGHYTYSENR^{145}	1801.75	$(909.82)^{2+}$ $(606.91)^{3+}$	1 met sulfoxide
	^{133}**MM**NGGHYTYSENR^{145}	1558.63	$(788.30)^{2+}$	1 met sulfoxide
	^{133}**MM**NGGHYTYSENRVEK^{148}	1914.84	$(966.40)^{2+}$ $(644.61)^{3+}$	1 met sulfoxide

[a] The numbering is for DJ-1 without a histidine tag. Cysteine and methionine residues are shown in bold type.

peratures than the wild-type protein. These findings are consistent with a report that the α-helical structure of recombinant E64D is more thermally stable than that of wild-type DJ-1 (*56*). IEF and LC-MS/MS data suggest that the increased stability of E64D is not due to an obvious decrease in oxidation during expression and purification. It is surprising that E64D exhibits somewhat reduced stability than wild-type DJ-1 upon thermal or urea-induced unfolding, given the evidence from ultracentrifugation data that E64D forms a more stable dimer. The reasons for this discrepancy are unclear. As one possibility, wild-type DJ-1 may be more kinetically stable than E64D, and this difference could partially mask the enhanced thermodynamic stability of E64D (especially in the case of the temperature ramp). Alternatively, the discrepancy could be due to the fact that the sedimentation and denaturation analyses monitor different molecular transitions (i.e., folded dimer to folded monomer vs folded dimer to unfolded monomer, respectively).

Importantly, our results show that two pathogenic substitutions (M26I and E64D) have strikingly different effects on DJ-1 structure and stability. Unlike M26, E64 is not conserved across vertebrates (e.g., rat DJ-1 has a glutamine residue at position 64), suggesting that it may be less critical for stabilizing the structure of DJ-1 (*55*). The crystal structure of wild-type DJ-1 reveals that E64 is located at the C-terminal end of α-helix B, a region that is apparently remote from the dimer interface (*25*−*29*). Additionally, the three-dimensional structure of E64D is nearly identical to that of the wild-type protein (*8*). Given these observations, it is unclear how the E64D substitution disrupts DJ-1 structure and function in patients with familial PD. As with other DJ-1 mutations linked to familial PD, the E64D substitution is rare (*8*), and, therefore, one must consider the possibility that the mutation is non-pathogenic. However, data obtained in a primary cell-culture model in our laboratory suggest that E64D has a reduced ability to protect dopaminergic neurons from various PD-related stresses (Liu et al., unpublished work), implying that the substitution may, in fact, disrupt DJ-1 function. As one possibility, the increased thermodynamic stability of E64D may perturb dynamic properties of DJ-1 that enable the protein to bind mitochondria (*18*) or act as a chaperone (*23*, *24*) in response to a redox switch. Alternatively, the E64D substitution may cause a loss of function via a mechanism unrelated to effects on protein dynamics (e.g., by disrupting interactions between DJ-1 and a binding partner).

Wild-Type DJ-1 Is Destabilized by Over-Oxidation. Our sedimentation-equilibrium data suggest that over-oxidation causes DJ-1 dimer destabilization, resulting in subunit dissociation and aggregation. In support of this idea, over-oxidized wild-type DJ-1 fails to undergo cooperative unfolding at high temperatures, similar to M26I. The reduced absolute ellipticity of over-oxidized DJ-1 suggests that over-oxidation elicits partial unfolding and/or a net conversion of α-helix to *β*-sheet (*53*, *54*), although the decreased signal may also result from light scattering by oxidized oligomers. Our data are consistent with recent findings that wild-type DJ-1 forms soluble oligomers under conditions of oxidation and heating (*24*).

The destabilization and aggregation of DJ-1 upon treatment with H_2O_2 may be due to the disruption of hydrophobic, polar, and hydrogen-bonding interactions that stabilize the protein (*57*, *58*). In contrast to our findings, Fink and colleagues (*24*) reported that exposure of DJ-1 to a 10-fold molar excess of H_2O_2 resulted in the conversion of C106 to sulfinic acid, without additional modifications and with no impact on the protein's secondary structure. One reason for the greater degree of oxidation observed in our study may

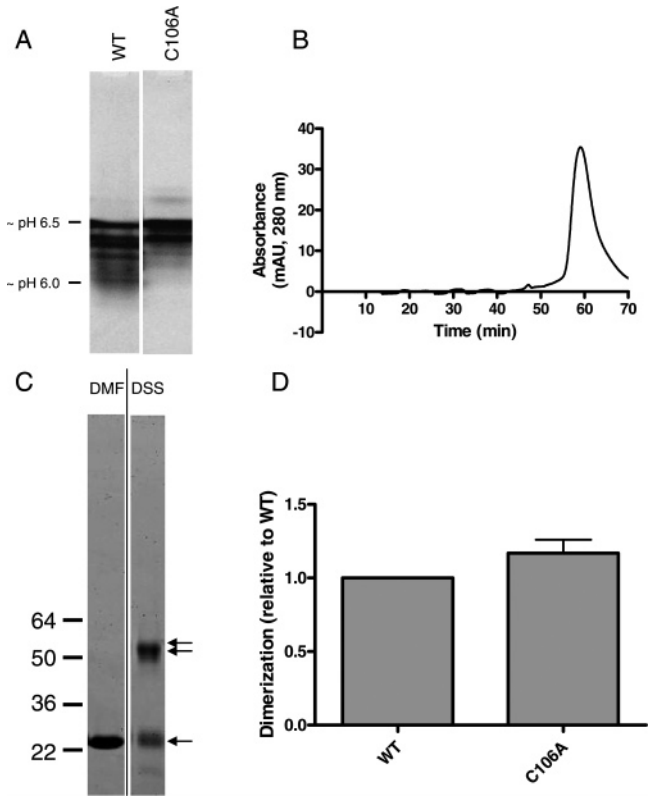

FIGURE 7: Wild-type DJ-1 and C106A have similar dimerization propensities. (A) Native IEF gel (pH range 3−7) showing that C106A consists of fewer acidic species than wild-type DJ-1. The pI values of IEF standards are shown to the left of the gel. (B) Quaternary structure of C106A determined by SEC. C106A (125 μL, 1 mg/mL) was injected on a Superdex 200 (10/30) column and eluted with PBS at a flow rate of 0.25 mL/min. (C) Extent of dimerization monitored by chemical cross-linking. C106A (10 μL, 0.2 mg/mL) was treated with DMF (vehicle control) or the primary amine cross-linker DSS and analyzed by electrophoresis on a 4−20% SDS−PAGE gel with Coomassie Blue staining. Double solid arrow: dimeric DJ-1; single solid arrow: monomeric DJ-1. Molecular weight markers are shown to the left of the gel. (D) Quantification of the extent of dimerization. The relative dimerization of C106A was determined by dividing the chemifluorescent signal for the cross-linked dimer (DSS lane) by the signal for the uncross-linked monomer (DMF lane). The data are plotted as the amount relative to the wild-type dimer level. The difference in dimerization between wild-type DJ-1 and C106A was not significant.

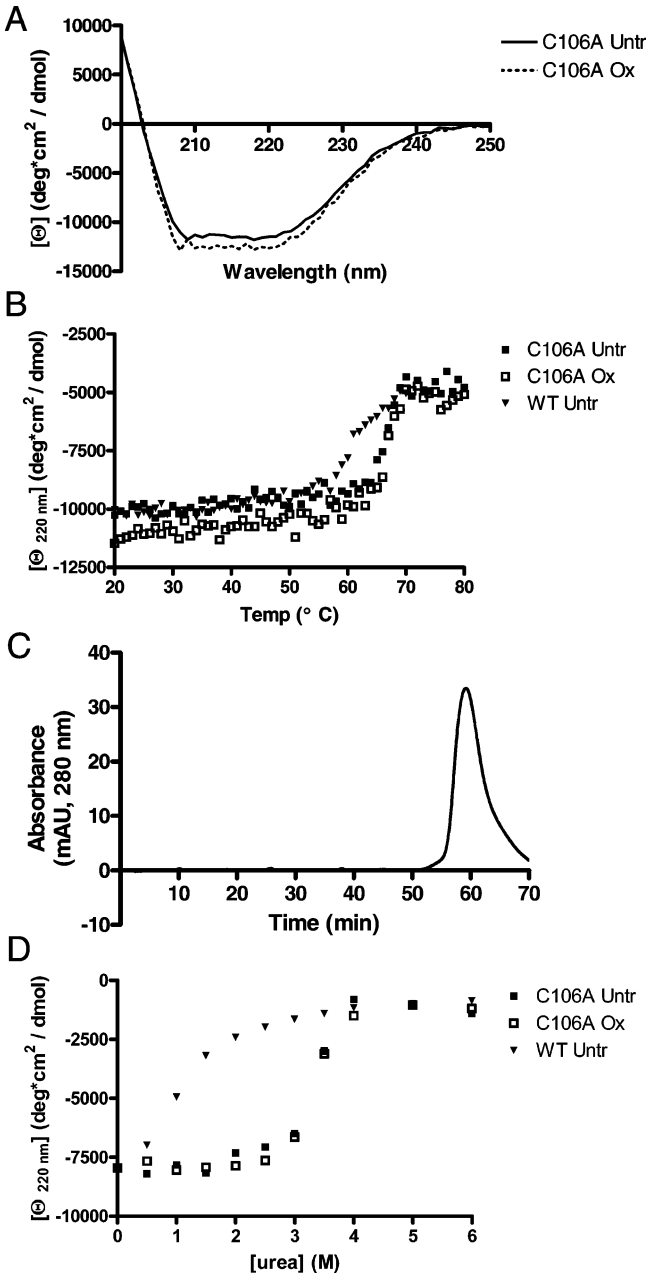

FIGURE 8: C106A is resistant to the destabilizing effects of oxidation and heating. (A) Secondary structure of untreated or over-oxidized C106A (3 μM) determined by far-UV CD. (B) Thermal unfolding of untreated or over-oxidized C106A (3 μM) monitored by far-UV CD. Ellipticity was measured at 220 nm with heating at a rate of 5 °C/min over a range of 20−80 °C. Data for untreated wild-type DJ-1 (from Figure 5B) are included for comparison. (C) Heat-induced unfolding and aggregation monitored by SEC. C106A (125 μL, 1 mg/mL) was incubated at 42 °C for 1 h and eluted from a Superdex 200 (10/30) column with PBS at a flow rate of 0.25 mL/min. (D) Urea-induced unfolding of untreated wild-type DJ-1, untreated C106A, or over-oxidized C106A (3 μM) monitored by far-UV CD. Each variant was incubated overnight at 22 °C in phosphate buffer containing various amounts of urea (0−6 M), and ellipticity was measured at 220 nm.

be that our DJ-1 preparations were more extensively oxidized even before treatment with H_2O_2 because of oxidation of the protein during expression and purification. Importantly, however, the degree of oxidation of our DJ-1 preparations (both before and after exposure to H_2O_2) are likely to be physiologically relevant, given that DJ-1 exhibits similar patterns of oxidative modification in the brains of sporadic PD patients and age-matched controls (*36*, *37*).

Our results have important implications for understanding PD pathogenesis. Wild-type DJ-1 undergoes more extensive oxidative modifications in the brains of sporadic PD patients than in age-matched controls (*36*), and the oxidation of DJ-1 increases with age in flies, mice, and humans (*37*). These findings, together with our results showing that oxidation causes DJ-1 destabilization and aggregation, suggest that functional impairment of wild-type DJ-1 due to oxidative damage contributes to neurodegeneration in sporadic PD.

Oxidation at C106 Contributes to DJ-1 Destabilization. Although C106A and wild-type DJ-1 are nearly identical in terms of secondary and quaternary structure, our results show that C106A is thermodynamically much more stable than the wild-type protein ($\Delta[\Delta G_u^{H_2O}]_{app} = 16 \pm 5$ kcal/mol), and C106A has a lower propensity to aggregate at elevated temperatures. In addition, sedimentation data obtained for

C106A fit best to a dimer model, implying that the mutant has a weaker propensity to undergo subunit dissociation than wild-type DJ-1. It would seem unlikely that the markedly enhanced stability of C106A is due to structural consequences of the cysteine-to-alanine substitution *per se*, given that this type of replacement is often destabilizing (see, for example, refs 59 and 60). Instead, we infer that the oxidation of C106 during expression and purification destabilizes the wild-type protein and, therefore, that C106A has enhanced stability because it is not susceptible to oxidative modification at position 106. In support of this idea, other groups have reported that DJ-1 undergoes facile oxidation at C106 during purification (*24*) or preparation for X-ray analysis (*29*). Moreover, our IEF results indicate that untreated C106A consists of fewer acidic isoforms than the untreated wild-type protein, and our LC-MS/MS data reveal that C106A is oxidized at many of the same sites as wild-type DJ-1 except for position 106. We also show that C106A is not destabilized upon over-oxidation by H_2O_2, in contrast to the wild-type protein. All of these findings suggest that C106 oxidation is necessary for destabilization of the wild-type protein, although it may not be *sufficient* for destabilization because residues other than C106 are also oxidized during expression and purification (Table 3) and upon H_2O_2 treatment (*24*). Our observation that C106A has enhanced stability differs from previous results showing that wild-type DJ-1 and C106A exhibit similar thermal denaturation profiles (*30*). The reasons for this discrepancy are uncertain, although it may be that our preparations of DJ-1 were oxidized more extensively during expression and purification than those described in the earlier study.

Previous reports have shown that substituting C106 with alanine or serine causes a disruption of antioxidant function (*18*, *32*). Other studies have suggested that the oxidation of C106 to sulfinic acid is part of a sensing mechanism in which DJ-1 responds to oxidative modification. This mechanism is critical for the ability of DJ-1 to respond to oxidative stress by binding to mitochondria (*18*) or by suppressing α-synuclein fibrillization via a chaperone mechanism (*24*). The oxidation of C106 to sulfonic acid leads to a loss of chaperone function, suggesting that tight regulation of the oxidation state of C106 is essential for DJ-1 function (*24*). These observations, together with our finding that C106A is more stable than the wild-type protein, raise an intriguing question: if the oxidation of C106 is critical for modulating DJ-1 function, then why does this modification induce DJ-1 destabilization? A key point in addressing this question is that the modification of C106 to the sulfinic acid is favored by hydrogen bonding (e.g., with E18) and, therefore, is expected to be functionally relevant (*18*, *29*). In contrast, a sulfonic acid at C106 would not be held stable by local hydrogen bonding and, therefore, would be predicted to cause a loss of function. The implication of our data is that there is a penalty associated with the oxygen-sensing function of DJ-1, namely, the protein is vulnerable to destabilization upon over-oxidation of C106 to the sulfonic acid, combined with oxidative modifications elsewhere on the polypeptide chain. Presumably, this structural penalty is tolerated early in life when ROS levels are relatively low, whereas it may lead to significant DJ-1 unfolding and inactivation under conditions of elevated oxidative stress in the brains of elderly individuals (*37*, *61*).

CONCLUSION

In summary, we provide evidence that the familial DJ-1 mutant M26I and the over-oxidized wild-type protein adopt unstable structures with a high propensity to form aggregates. The M26I substitution may be especially destabilizing when combined with oxidative modifications elsewhere on the polypeptide chain. In contrast to M26I, E64D adopts a stable dimeric structure similar to that of wild-type DJ-1, indicating that not all familial substitutions cause DJ-1 destabilization. Although the conversion of C106 to the sulfinic acid is apparently essential for the oxidative-stress-sensing mechanism of DJ-1, oxidation of this residue also contributes to DJ-1 destabilization. Our data suggest that DJ-1 may be inactivated by over-oxidation during aging, and this age-dependent inactivation may play a role in neurodegeneration. From these results, we suggest that therapies aimed at stabilizing dimeric DJ-1 and suppressing DJ-1 oxidation may be beneficial for treating PD.

ACKNOWLEDGMENT

We are grateful to Aaron Craft and Katherine Jungbluth for technical assistance with preparing DJ-1 expression constructs. We also thank Dr. Chiwook Park for reading the manuscript and providing insightful suggestions.

SUPPORTING INFORMATION AVAILABLE

A diagram of the predicted secondary structure for wild-type DJ-1, M26I, and E64D is provided. This material is available free of charge via the Internet at http://pubs.acs.org.

REFERENCES

1. Dawson, T. M., and Dawson, V. L. (2002) Neuroprotective and neurorestorative strategies for Parkinson's disease, *Nat. Neurosci. Suppl. 5*, 1058−1061.
2. Spillantini, M. G., Schmidt, M. L., Lee, V. M.-Y., Trojanowski, J. Q., Jakes, R., and Goedert, M. (1997) α-Synuclein in Lewy bodies, *Nature 388*, 839−840.
3. Sherer, T. B., Betarbet, R., Stout, A. K., Lund, S., Baptista, M., Panov, A. V., Cookson, M. R., and Greenamyre, J. T. (2002) An in vitro model of Parkinson's disease: linking mitochondrial impairment to altered α-synuclein metabolism and oxidative damage, *J. Neurosci. 22*, 7006−7015.
4. Jenner, P. (1998) Oxidative mechanisms in nigral cell death in Parkinson's disease, *Mov. Disord. Suppl. 1 13*, 24−34.
5. Orth, M., and Schapira, A. H. (2002) Mitochondrial involvement in Parkinson's disease, *Neurochem. Int. 40*, 533−541.
6. Bonifati, V., Rizzu, P., van Baren, M. J., Schaap, O., Breedveld, G. J., Krieger, E., Dekker, M. C., Squitieri, F., Ibanez, P., Joosse, M., van Dongen, J. W., Vanacore, N., van Swieten, J. C., Brice, A., Meco, G., van Duijn, C. M., Oostra, B. A., and Heutink, P. (2003) Mutations in the DJ-1 gene associated with autosomal recessive early-onset parkinsonism, *Science 299*, 256−259.
7. Abou-Sleiman, P. M., Healy, D. G., Quinn, N., Lees, A. J., and Wood, N. W. (2003) The role of pathogenic DJ-1 mutations in Parkinson's disease, *Ann. Neurol. 54*, 283−286.
8. Hering, R., Strauss, K. M., Tao, X., Bauer, A., Woitalla, D., Mietz, E. M., Petrovic, S., Bauer, P., Schaible, W., Muller, T., Schols, L., Klein, C., Berg, D., Meyer, P. T., Schulz, J. B., Wollnik, B., Tong, L., Kruger, R., and Riess, O. (2004) Novel homozygous p.E64D mutation in DJ1 in early onset Parkinson disease (PARK7), *Hum. Mutat. 24*, 321−329.
9. Yokota, T., Sugawara, K., Ito, K., Takahashi, R., Ariga, H., and Mizusawa, H. (2003) Down regulation of DJ-1 enhances cell death by oxidative stress, ER stress, and proteasome inhibition, *Biochem. Biophys. Res. Commun. 312*, 1342−1348.
10. Taira, T., Saito, Y., Niki, T., Iguchi-Ariga, S. M., Takahashi, K., and Ariga, H. (2004) DJ-1 has a role in antioxidative stress to prevent cell death, *EMBO Rep. 5*, 213−218.

11. Chen, L., Cagniard, B., Mathews, T., Jones, S., Koh, H. C., Ding, Y., Carvey, P. M., Ling, Z., Kang, U. J., and Zhuang, X. (2005) Age-dependent motor deficits and dopaminergic dysfunction in DJ-1 null mice, *J. Biol. Chem. 280*, 21418−21426.
12. Goldberg, M. S., Pisani, A., Haburcak, M., Vortherms, T. A., Kitada, T., Costa, C., Tong, Y., Martella, G., Tscherter, A., Martins, A., Bernardi, G., Roth, B. L., Pothos, E. N., Calabresi, P., and Shen, J. (2005) Nigrostriatal dopaminergic deficits and hypokinesia caused by inactivation of the familial Parkinsonism-linked gene DJ-1, *Neuron 45*, 489−496.
13. Kim, R. H., Smith, P. D., Aleyasin, H., Hayley, S., Mount, M. P., Pownall, S., Wakeham, A., You-Ten, A. J., Kalia, S. K., Horne, P., Westaway, D., Lozano, A. M., Anisman, H., Park, D. S., and Mak, T. W. (2005) Hypersensitivity of DJ-1-deficient mice to 1-methyl-4-phenyl-1,2,3,6-tetrahydropyrindine (MPTP) and oxidative stress, *Proc. Natl. Acad. Sci. U.S.A. 102*, 5215−5220.
14. Menzies, F. M., Yenisetti, S. C., and Min, K. T. (2005) Roles of Drosophila DJ-1 in survival of dopaminergic neurons and oxidative stress, *Curr. Biol. 15*, 1578−1582.
15. Meulener, M., Whitworth, A. J., Armstrong-Gold, C. E., Rizzu, P., Heutink, P., Wes, P. D., Pallanck, L. J., and Bonini, N. M. (2005) Drosophila DJ-1 mutants are selectively sensitive to environmental toxins associated with Parkinson's disease, *Curr. Biol. 15*, 1572−1577.
16. Yang, Y., Gehrke, S., Haque, M. E., Imai, Y., Kosek, J., Yang, L., Beal, M. F., Nishimura, I., Wakamatsu, K., Ito, S., Takahashi, R., and Lu, B. (2005) Inactivation of Drosophila DJ-1 leads to impairments of oxidative stress response and phosphatidylinositol 3-kinase/Akt signaling, *Proc. Natl. Acad. Sci. U.S.A. 102*, 13670−13675.
17. Mitsumoto, A., Nakagawa, Y., Takeuchi, A., Okawa, K., Iwamatsu, A., and Takanezawa, Y. (2001) Oxidized forms of peroxiredoxins and DJ-1 on two-dimensional gels increased in response to sublethal levels of paraquat, *Free Radical Res. 35*, 301−310.
18. Canet-Aviles, R. M., Wilson, M. A., Miller, D. W., Ahmad, R., McLendon, C., Bandyopadhyay, S., Baptista, M. J., Ringe, D., Petsko, G. A., and Cookson, M. R. (2004) The Parkinson's disease protein DJ-1 is neuroprotective due to cysteine-sulfinic acid-driven mitochondrial localization, *Proc. Natl. Acad. Sci. U.S.A. 101*, 9103−9108.
19. Kinumi, T., Kimata, J., Taira, T., Ariga, H., and Niki, E. (2004) Cysteine-106 of DJ-1 is the most sensitive cysteine residue to hydrogen peroxide-mediated oxidation in vivo in human umbilical vein endothelial cells, *Biochem. Biophys. Res. Commun. 317*, 722−728.
20. Betarbet, R., Canet-Aviles, R. M., Sherer, T. B., Mastroberardino, P. G., McLendon, C., Kim, J. H., Lund, S., Na, H. M., Taylor, G., Bence, N. F., Kopito, R., Seo, B. B., Yagi, T., Yagi, A., Klinefelter, G., Cookson, M. R., and Greenamyre, J. T. (2006) Intersecting pathways to neurodegeneration in Parkinson's disease: effects of the pesticide rotenone on DJ-1, alpha-synuclein, and the ubiquitin-proteasome system, *Neurobiol. Dis. 22*, 404−420.
21. Blackinton, J., Ahmad, R., Miller, D. W., van der Brug, M. P., Canet-Aviles, R. M., Hague, S. M., Kaleem, M., and Cookson, M. R. (2005) Effects of DJ-1 mutations and polymorphisms on protein stability and subcellular localization, *Brain Res. Mol. Brain Res. 134*, 76−83.
22. Zhang, L., Shimoji, M., Thomas, B., Moore, D. J., Yu, S. W., Marupudi, N. I., Torp, R., Torgner, I. A., Ottersen, O. P., Dawson, T. M., and Dawson, V. L. (2005) Mitochondrial localization of the Parkinson's disease related protein DJ-1: implications for pathogenesis, *Hum. Mol. Genet. 14*, 2063−2073.
23. Shendelman, S., Jonason, A., Martinat, C., Leete, T., and Abeliovich, A. (2004) DJ-1 is a redox-dependent molecular chaperone that inhibits alpha-synuclein aggregate formation, *PLoS Biol. 2*, e362.
24. Zhou, W., Zhu, M., Wilson, M. A., Petsko, G. A., and Fink, A. L. (2006) The oxidation state of DJ-1 regulates its chaperone activity toward alpha-synuclein, *J. Mol. Biol. 356*, 1036−1048.
25. Honbou, K., Suzuki, N. N., Horiuchi, M., Niki, T., Taira, T., Ariga, H., and Inagaki, F. (2003) The crystal structure of DJ-1, a protein related to male fertility and Parkinson's disease, *J. Biol. Chem. 278*, 31380−31384.
26. Huai, Q., Sun, Y., Wang, H., Chin, L. S., Li, L., Robinson, H., and Ke, H. (2003) Crystal structure of DJ-1/RS and implication on familial Parkinson's disease, *FEBS Lett. 549*, 171−175.
27. Lee, S. J., Kim, S. J., Kim, I. K., Ko, J., Jeong, C. S., Kim, G. H., Park, C., Kang, S. O., Suh, P. G., Lee, H. S., and Cha, S. S. (2003) Crystal structures of human DJ-1 and *Escherichia coli* Hsp31, which share an evolutionarily conserved domain, *J. Biol. Chem. 278*, 44552−44559.
28. Tao, X., and Tong, L. (2003) Crystal structure of human DJ-1, a protein associated with early onset Parkinson's disease, *J. Biol. Chem. 278*, 31372−31379.
29. Wilson, M. A., Collins, J. L., Hod, Y., Ringe, D., and Petsko, G. A. (2003) The 1.1-A resolution crystal structure of DJ-1, the protein mutated in autosomal recessive early onset Parkinson's disease, *Proc. Natl. Acad. Sci. U.S.A. 100*, 9256−9261.
30. Olzmann, J. A., Brown, K., Wilkinson, K. D., Rees, H. D., Huai, Q., Ke, H., Levey, A. I., Li, L., and Chin, L. S. (2004) Familial Parkinson's disease-associated L166P mutation disrupts DJ-1 protein folding and function, *J. Biol. Chem. 279*, 8506−8515.
31. Moore, D. J., Zhang, L., Dawson, T. M., and Dawson, V. L. (2003) A missense mutation (L166P) in DJ-1, linked to familial Parkinson's disease, confers reduced protein stability and impairs homo-oligomerization, *J. Neurochem. 87*, 1558−1567.
32. Takahashi-Niki, K., Niki, T., Taira, T., Iguchi-Ariga, S. M., and Ariga, H. (2004) Reduced anti-oxidative stress activities of DJ-1 mutants found in Parkinson's disease patients, *Biochem. Biophys. Res. Commun. 320*, 389−397.
33. Junn, E., Taniguchi, H., Jeong, B. S., Zhao, X., Ichijo, H., and Mouradian, M. M. (2005) Interaction of DJ-1 with Daxx inhibits apoptosis signal-regulating kinase 1 activity and cell death, *Proc. Natl. Acad. Sci. U.S.A. 102*, 9691−9696.
34. Macedo, M. G., Anar, B., Bronner, I. F., Cannella, M., Squitieri, F., Bonifati, V., Hoogeveen, A., Heutink, P., and Rizzu, P. (2003) The DJ-1L166P mutant protein associated with early onset Parkinson's disease is unstable and forms higher-order protein complexes, *Hum. Mol. Genet. 12*, 2807−2816.
35. Baulac, S., LaVoie, M. J., Strahle, J., Schlossmacher, M. G., and Xia, W. (2004) Dimerization of Parkinson's disease-causing DJ-1 and formation of high molecular weight complexes in human brain, *Mol. Cell. Neurosci. 27*, 236−246.
36. Choi, J., Sullards, M. C., Olzmann, J. A., Rees, H. D., Weintraub, S. T., Bostwick, D. E., Gearing, M., Levey, A. I., Chin, L. S., and Li, L. (2006) Oxidative damage of DJ-1 is linked to sporadic Parkinson and Alzheimer diseases, *J. Biol. Chem. 281*, 10816−10824.
37. Meulener, M. C., Xu, K., Thompson, L., Ischiropoulos, H., and Bonini, N. M. (2006) Mutational analysis of DJ-1 in Drosophila implicates functional inactivation by oxidative damage and aging, *Proc. Natl. Acad. Sci. U.S.A. 103*, 12517−12522.
38. Laue, T. M., and Stafford, W. F., III. (1999) Modern applications of analytical ultracentrifugation, *Annu. Rev. Biophys. Biomol. Struct. 28*, 75−100.
39. Johnson, M. L., Correia, J. J., Yphantis, D. A., and Halvorson, H. R. (1981) Analysis of data from the analytical ultracentrifuge by nonlinear least-squares techniques, *Biophys. J. 36*, 575−588.
40. Laue, T. M., Shah, B. D., Ridgeway, T. M., and Pelletier, S. L. (1992) *Analytical Ultracentrifugation in Biochemistry and Polymer Science*, (Harding, S., and Rowe, A., Eds.) pp 90−125, Royal Society of Chemistry, London, England.
41. Pace, C. N. (1975) The stability of globular proteins, *CRC Crit. Rev. Biochem. 3*, 1−43.
42. Pace, C. N. (1986) Determination and analysis of urea and guanidine hydrochloride denaturation curves, *Methods Enzymol. 131*, 266−280.
43. Bowie, J. U., and Sauer, R. T. (1989) Equilibrium dissociation and unfolding of the Arc repressor dimer, *Biochemistry 28*, 7139−7143.
44. Shortle, D. (1989) Probing the determinants of protein folding and stability with amino acid substitutions, *J. Biol. Chem. 264*, 5315−5318.
45. Rochet, J. C., Brownie, E. R., Oikawa, K., Hicks, L. D., Fraser, M. E., James, M. N., Kay, C. M., Bridger, W. A., and Wolodko, W. T. (2000) Pig heart CoA transferase exists as two oligomeric forms separated by a large kinetic barrier, *Biochemistry 39*, 11291−11302.
46. De Francesco, R., Pastore, A., Vecchio, G., and Cortese, R. (1991) Circular dichroism study on the conformational stability of the dimerization domain of transcription factor LFB1, *Biochemistry 30*, 143−147.
47. Milla, M. E., Brown, B. M., and Sauer, R. T. (1993) P22 Arc repressor: enhanced expression of unstable mutants by addition of polar C-terminal sequences, *Protein Sci. 2*, 2198−2205.

48. Myers, J. K., Pace, C. N., and Scholtz, J. M. (1995) Denaturant m values and heat capacity changes: relation to changes in accessible surface areas of protein unfolding, *Protein Sci. 4*, 2138−2148.
49. Mok, Y. K., de Prat Gay, G., Butler, P. J., and Bycroft, M. (1996) Equilibrium dissociation and unfolding of the dimeric human papillomavirus strain-16 E2 DNA-binding domain, *Protein Sci. 5*, 310−319.
50. Mirzaei, H., and Regnier, F. (2006) Identification and quantification of protein carbonylation using light and heavy isotope labeled Girard's P reagent, *J. Chromatogr., A 1134*, 122−133.
51. Perkins, D. N., Pappin, D. J., Creasy, D. M., and Cottrell, J. S. (1999) Probability-based protein identification by searching sequence databases using mass spectrometry data, *Electrophoresis 20*, 3551−3567.
52. Benitez-Cardoza, C. G., Rojo-Dominguez, A., and Hernandez-Arana, A. (2001) Temperature-induced denaturation and renaturation of triosephosphate isomerase from *Saccharomyces cerevisiae*: evidence of dimerization coupled to refolding of the thermally unfolded protein, *Biochemistry 40*, 9049−9058.
53. Woody, R. W. (1995) Circular dichroism, *Methods Enzymol. 246*, 34−71.
54. Sreerama, N., and Woody, R. W. (2004) Computation and analysis of protein circular dichroism spectra, *Methods Enzymol. 383*, 318−351.
55. Bandyopadhyay, S., and Cookson, M. R. (2004) Evolutionary and functional relationships within the DJ1 superfamily, *BMC Evol. Biol. 4*, 6.
56. Gorner, K., Holtorf, E., Odoy, S., Nuscher, B., Yamamoto, A., Regula, J. T., Beyer, K., Haass, C., and Kahle, P. J. (2003) Differential effects of Parkinson's disease-associated mutations on stability and folding of DJ-1, *J. Biol. Chem. 279*, 6943−6951.
57. Chapman, A. L., Winterbourn, C. C., Brennan, S. O., Jordan, T. W., and Kettle, A. J. (2003) Characterization of non-covalent oligomers of proteins treated with hypochlorous acid, *Biochem. J. 375*, 33−40.
58. Wood, Z. A., Schroder, E., Robin Harris, J., and Poole, L. B. (2003) Structure, mechanism and regulation of peroxiredoxins, *Trends Biochem. Sci. 28*, 32−40.
59. Senga, T., Miyazaki, K., Machida, K., Iwata, H., Matsuda, S., Nakashima, I., and Hamaguchi, M. (2000) Clustered cysteine residues in the kinase domain of v-Src: critical role for protein stability, cell transformation and sensitivity to herbimycin A, *Oncogene 19*, 273−279.
60. Bondar, V. S., Purtov, K. V., Malikova, N. P., Frank, L. A., and Illarionov, B. A. (2001) Role of conservative residue Cys158 in the formation of an active photoprotein complex of obelin, *Biochemistry (Moscow) 66*, 1014−1018.
61. Squier, T. C. (2001) Oxidative stress and protein aggregation during biological aging, *Exp. Gerontol. 36*, 1539−1550.
62. Garnier, J., Osguthorpe, D. J., and Robson, B. (1978) Analysis of the accuracy and implications of simple methods for predicting the secondary structure of globular proteins, *J. Mol. Biol. 120*, 97−120.

BI7001778